GEOPHYSICAL RESEARCH LETTERS, VOL. 28, NO. 12, PAGES 2297-2300, JUNE 15, 2001

Laboratory results indicating complex and potentially unstable frictional behavior of smectite clay

Demian M. Saffer

Department of Geology and Geophysics, University of Wyoming, Laramie WY

Kevin M. Frye, Chris Marone[1], Karen Mair[2]

Department of Earth, Atmospheric, and Planetary Sciences, MIT, Cambridge MA

Abstract. A central problem in explaining the apparent weakness of the San Andreas and other plate boundary faults has been identifying candidate fault zone materials that are both weak and capable of hosting earthquake-like unstable rupture. Our results demonstrate that smectite clay can be both weak and velocity weakening at low normal stress (<30 MPa). Our data are consistent with previous work, which has focused on higher normal stress conditions (50 MPa and greater) and found only velocity strengthening. If natural fault zones contain significant smectite, one key implication of our results is that localized zones of high pore pressure, which reduce effective normal stress, could be important in controlling potential sites of earthquake nucleation. Our experiments indicate that friction of smectite is complex, and depends upon both sliding velocity and normal stress. This complexity highlights the need for detailed experiments that reflect in-situ conditions for fault gouges.

Introduction

A growing body of geophysical, geological, and seismological evidence demonstrates that many plate boundary faults, in both subduction zone and continental transform settings, support considerably lower shear stresses than predicted by laboratory-derived friction laws for crustal rocks. These data include inferred stress orientations [e.g. *Zoback et al.*, 1987], and constraints on shear stress magnitude estimated from heat flow measurements [e.g., *Brune and Roy*, 1969]. Proposed explanations for the discrepancy between observations and the known frictional properties of geologic materials, known as the "stress-heat flow paradox", include (1) the presence of low-friction clay or serpentinite gouge lining the fault, and (2) the maintenance of elevated pore pressure localized within the fault zone [e.g., *Rice*, 1992].

A long-standing problem in explaining the apparent weakness of mature faults with hypothesis (1) above has been identifying candidate materials that are both weak and capable of hosting earthquake-like unstable rupture [e.g., *Scholz*, 1998]. Existing experimental data indicate that some clay and serpentine minerals may be sufficiently weak, but all exhibit velocity-strengthening frictional behavior (frictional strength increases with slip velocity), which produces only stable slip. Alternatively, hypothesis (2) above requires a mechanism for generating extremely localized and persistent elevated pore pressure within the fault; it is unclear whether any known mechanisms are hydrologically or mechanically viable [e.g., *Rice*, 1992]. A second problem with this hypothesis is that dilatancy would tend to stabilize rupture by dynamically decreasing pore pressure [e.g., *Segall and Rice*, 1995], thus making it difficult to explain a fault that is both weak and seismogenic. In clay-rich gouges, temperature- and pressure-induced dehydration [e.g., *Fitts and Brown*, 1999] combined with low permeability may result in elevated pore pressures. Thus, it is likely that a combination of hypotheses (1) and (2) apply to mature fault zones.

Clay minerals, and smectites in particular, are a common product of mechanical and chemical weathering. As a result, high smectite abundance is often observed in fault gouge [e.g., *Vrolijk & Van Der Pluijm*, 1999]; thus, a considerable body of experimental work has focused on investigating its frictional properties [e.g., *Wang et al.*, 1980; *Shimamoto and Logan*, 1981; *Logan and Rauenzahn*, 1987; *Morrow et al*, 1992, 2000]. Smectite may persist as a major component of fault gouge to several km depth, below which a thermally-driven transformation to illite occurs [e.g., *Colten-Bradley*, 1987]. The depth of this transformation depends primarily upon thermal conditions and is usually complete by temperatures of 150° C [e.g., *Bird*, 1984]. Despite the potential importance of smectite in controlling the frictional properties of faults, previous work has focused on its velocity-dependent frictional properties at effective normal stresses above 50 MPa, and over a limited range of sliding velocities. Low effective stresses are expected if fault weakness is due, in part, to locally elevated pore pressure. In addition, a comprehensive examination of frictional velocity-dependence of clay minerals has been lacking. To investigate the frictional properties of smectite over a range of normal stresses and sliding velocities, we conducted a series of velocity-stepping direct shear experiments on pure Ca-smectite gouge.

Experimental Methods

In all experiments, we sheared layers of commercially obtained Ca-smectite powder (grain size ranging from 2-500 μm) in the double-direct shear geometry (Figure 1a, inset) to displacements of 20-28 mm (shear strains of ~6-8) at room humidity and temperature. Gouge layers were made by

[1]Now at Department of Geosciences, Pennsylvania State University, University Park.

[2]Now at Department of Earth Sciences, University of Liverpool, Liverpool L69 3GP, UK.

Paper number 2001GL012869
0094-8276/01/2001GL012869$05.00

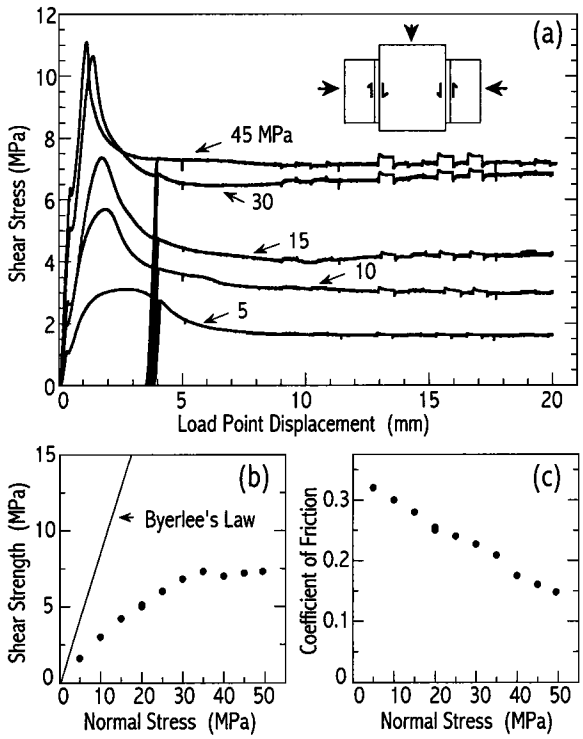

Figure 1. (a) Shear stress versus load point displacement for 3-mm thick layers of smectite gouge sheared at normal stresses of 5, 10, 15, 30, and 45 MPa. The initial portion of each experiment included an unloading-reloading cycle at 4 mm displacement. Note the pronounced peak stress and weakening in the first few mm of displacement. With increasing normal stress the magnitude of the peak stress increases and displacement required for subsequent weakening decreases. After 9 mm of displacement, sliding velocity was stepped between 1, 10, and 100 μm/s. Inset shows sketch of double-direct shear experimental geometry used for the experiments. (b) Sliding friction failure envelope calculated from measured shear stress at 20 mm displacement in all tests. Note the change in slope of the failure envelope at 30-35 MPa normal stress. Line for Byerlee's law ($\mu = 0.85$) is shown for comparison. (c) Coefficient of sliding friction at 20 mm displacement vs. normal stress. The reproducibility of data plotted in (b) and (c) is shown by results of multiple experiments at the same normal stress, which overlay in most cases.

smoothing the powder onto grooved steel forcing blocks in a leveling jig, and the initial thickness, precisely 5 mm prior to the application of normal load, was identical in each experiment. Initial compaction of the gouge upon loading under normal stress decreased layer thickness to approximately 3 mm in all cases. Layers were not subject to tamping or vibrations before being placed into the apparatus and loaded.

The smectite used in our experiments contained ~11% water by weight, as measured in samples prior to shearing. This is typical of Ca-smectite under conditions of room humidity and temperature, as determined from thermodynamic calculations and direct measurements of hydration state [e.g., *Bird*, 1984]. It may represent either fully hydrated single water interlayers (*Bird's* hydration phase Ih), or partially hydrated smectite with two water interlayers (*Bird's* hydration phase II-6). These hydration phases are expected to exist stably under in situ conditions to 6-10 km depth, for a geotherm of 20-25 °C/km [*Bird*, 1984]. Using unsaturated smectite allowed us to characterize the mechanical properties of the mineral, while minimizing the effect of transient pore pressure changes in a low-permeability gouge. However, it is important to note that adsorbed water has been shown to affect the frictional strength of smectite [e.g., *Morrow et al.*, 2000]. Ultimately, the frictional characteristics of the gouge material can be integrated with rupture models that treat transient pore water pressurization and volume change explicitly [e.g., *Segall and Rice*, 1995].

We investigated the velocity-dependence of sliding friction for velocities ranging from 0.2 to 200 μm/s and normal stresses from 5 to 50 MPa. Step changes in load point velocity resulted in a sharp change in shear strength, followed by a gradual decay to a new steady-state sliding friction for a given velocity (Figure 1a). Here, we define the upstep velocity as the higher of the two sliding velocities in each velocity-step experiment. The velocity dependence of sliding friction, $\mu = \tau/\sigma n$, where τ is shear stress at steady state and σn is normal stress, is reported as $(a\text{-}b) = \Delta\mu/\Delta \ln V$, where V is sliding velocity. Negative values of $(a\text{-}b)$ reflect velocity-weakening behavior, which can result in unstable or conditionally stable slip. Positive values of $(a\text{-}b)$ reflect velocity-strengthening, which results in stable sliding [e.g. *Marone*, 1998].

Experimental Results

In our experiments, sliding friction ranged from 0.14 to 0.30, and decreased with increasing normal stress (Figures 1a-c). These values are consistent with previous work on clays [e.g., *Morrow et al*, 1992, 2000]. The experimentally determined failure envelope changes slope at an effective normal stress of 35 MPa (Figure 1b), suggesting a transition away from dominantly brittle, pressure-sensitive deformation mechanisms with increasing normal stress.

Our strength data indicate a distinct peak and subsequent decay in shear stress during the first 4 mm of displacement

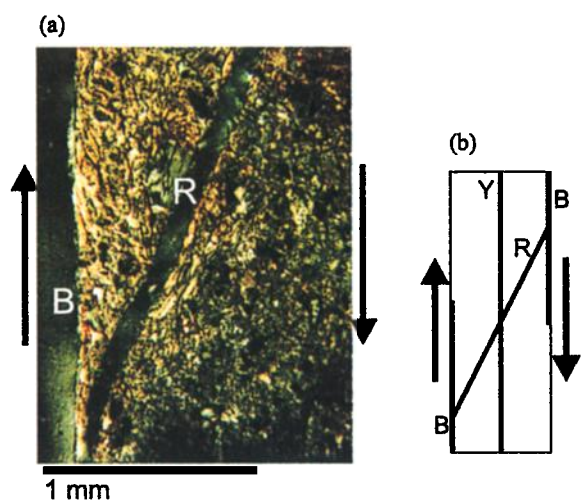

Figure 2. (a) Photomicrograph of sample deformed to a shear strain of 6 at 15 MPa normal stress, taken in cross-polarized light. Sense of shear is shown by the arrows. B and R denote interpreted boundary and Riedel shears, respectively. Note the strong alignment of clay grains (shown as bright areas) and the crack (opened during epoxy impregnation) that has formed along the structure interpreted as an R_1 Riedel shear band. (b) Generalized diagram of geometries typical in sheared gouge, where R is a Riedel shear, B are boundary shears, and Y is a boundary-parallel shear (modified from *Logan et al.*, 1979).

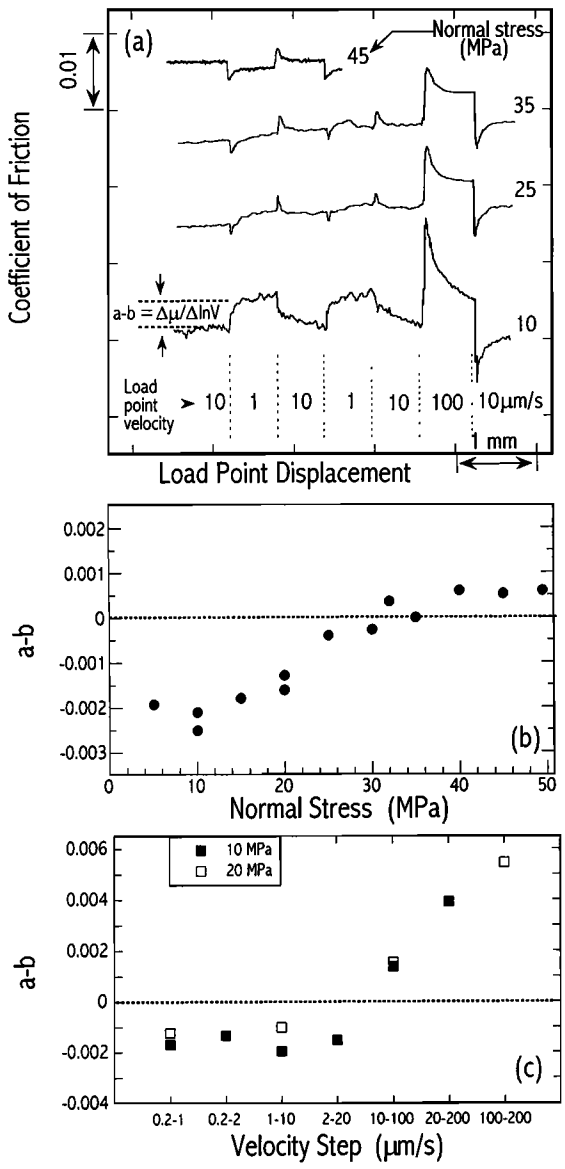

Figure 3. (a) Friction versus load-point displacement during velocity stepping at a range of normal stresses. Friction levels are arbitrary, see Figure 1 for absolute values; displacement starts at 18.0 mm. (b) Frictional velocity-dependence (a-b) as a function of normal stress for velocity-stepping tests from 1-10 μm/s, at 18-23 mm displacement. Note the transition from velocity-weakening (a-b < 0) to velocity-strengthening (a-b > 0) at 30-35 MPa. (c) Frictional velocity-dependence for different sliding velocities at normal stresses of 10 and 20 MPa. Values of (a-b) are from individual velocity steps; measurement precision is of order of the symbol size. Experimental reproducibility is shown by multiple values at the same normal stress. Frictional velocity dependence varies with absolute velocity and changes to velocity strengthening at higher velocities.

(Figure 1a). In general, steady-state sliding friction was reached after shear of < 6 mm. The initial stress-strain behavior varied strongly with normal stress; the magnitude of the initial peak stress increased with increased normal stress, whereas the displacement necessary to reach steady sliding friction decreased (Figure 1a).

Photomicrographs taken in cross-polarized light show development of shear-related fabric in experiments performed at 15 MPa normal stress and higher. Figure 2a shows an epoxy-filled crack, with aligned clay grains at its edges. In addition, several smaller parallel structures are imaged and appear as linear or nearly linear cracks. Based on their orientation, 20-25° to the edge of layer (i.e. the direction of imposed shear), we interpret these structures as Riedel shear bands (Figures 2a-b). Boundary-parallel shears are also present, and have aligned clay grains along their edges.

Our data for upstep sliding velocities <20 μm/s document a clear transition from velocity-weakening to velocity-strengthening at a normal stress of 30 MPa (Figures 3a-b). In contrast, for upstep sliding velocities >20 μm/s we observe velocity-strengthening over the entire range of normal stresses studied. At normal stresses below 30 MPa, (a-b) increases strongly with increased sliding velocity (Figure 3c). These effects are generally independent of displacement once steady-state friction has been reached.

Our observation of velocity strengthening at normal stresses above 30 MPa is consistent with previous work on clays. Existing studies have focused on effective normal stresses in the 50-100 MPa range and above and, although covering only a limited range of sliding velocities, show only velocity strengthening [e.g., *Morrow et al.*, 1992]. Maximum values for (a-b) of 0.0053 reported here for normal stresses >30 MPa and upstep velocities of 200 μm/s are similar to the value of 0.005 reported by *Morrow et al.* [1992] for effective normal stresses of 200 MPa. In addition, a transition to velocity-weakening in montmorillonite at low sliding velocities was hypothesized by *Logan and Rauenzahn* [1987], based on a trend of decreasing positive values of (a-b) with lower sliding velocities at a normal stress of 50 MPa. This behavior contrasts with that for quartz gouge, which shows that once quasi-steady state sliding is reached (by shear strains of 2-3), its frictional velocity-dependence does not vary with sliding velocity and varies only slightly with normal stress [*Mair and Marone*, 1999].

Discussion and Geologic Implications

The transition to pressure-insensitive deformation, observed at 30 MPa normal stress, occurs at a significantly lower normal stress than for other materials (quartz, carbonate, or granite, for example). *Bird* [1984] observed a similar departure from brittle, Coulomb failure at 10-40 MPa normal stress, and suggested it was controlled by the existence of a weak hydrated glide plane within the clay mineral structure. An alternative explanation is that stress-induced dehydration occurred during our experiment, expelling interlayer water into the intergranular pore space and resulting in undetected high pore pressures. However, we do not favor this explanation because existing laboratory and theoretical considerations indicate that stress-induced smectite dehydration of hydration phases I-h or II-6 at room temperature does not occur at normal stresses below 150 MPa [*Bird*, 1984: *Colten-Bradley*, 1987]. However, at this time it is not possible to rule out such a mechanism.

We suggest that the observed peak and subsequent decrease in frictional strength with continued displacement reflects shear-enhanced compaction and alignment of platy clay minerals during early stages of shearing. A peak and subsequent decrease in shear strength to a residual value with increased displacement is commonly observed in clays and clay-rich soils, and is interpreted to result from alignment of clay particles [e.g., *Lupini et al.*, 1981, *Chester and Logan*, 1987]. The development of preferred grain orientations along

the edges of shears (Figure 2) is consistent with the interpretation that clay mineral alignment occurs during shearing and is responsible for the peak and subsequent decay in observed shear stress with continued displacement. Additional experiments and further examination of microstructures at various stages of displacement will conclusively refute or support this hypothesis.

Our results indicate that the frictional behavior of smectite is complex and sensitive to both normal stress and sliding velocity. This is the first detailed investigation of smectite frictional properties over a range of normal stresses and sliding velocities, and raises the possibility that smectite may be both weak ($\mu<0.25$) and velocity-weakening (unstable) under certain conditions. At low sliding velocities (<20 μm/s) and low normal stresses (<30 MPa), smectite exhibits velocity-weakening behavior and its frictional strength is pressure dependent. At higher sliding velocities, and at high normal stresses, smectite is velocity-strengthening. Some serpentine minerals have been shown to follow a two-mechanism constitutive law that depends upon sliding velocity [*Reinen et al.*, 1994], and we suggest that the frictional behavior of smectite may be similarly complex. Notably, viscous behavior of both dry and saturated, drained smectite has been documented in laboratory triaxial and hydrostatic loading experiments at room temperature [*Hagin et al.*, 1999], and is consistent with our observation of pressure-insensitive strength under some conditions.

If our data can be applied to natural faults, a key implication is that smectite-rich fault zones may be both weak and host earthquake-like unstable rupture. The effect of normal stress on velocity-dependence suggests that at seismogenic depths, localized zones of high pore pressure, which reduce effective normal stress, could control the location of velocity-weakening zones and thus may be important in earthquake nucleation. At shallow depths, unstable behavior of mature fault zones [e.g., *Marone and Scholz*, 1988] may be limited by the presence of unconsolidated gouge, which exhibits velocity-strengthening frictional behavior and results in stable sliding [e.g., *Scholz*, 1998; *Marone*, 1998]. Our data demonstrate the sensitivity of frictional behavior to ambient conditions, and highlight the need for detailed experiments over a wider range of normal stresses, sliding velocities, (and potentially other factors, such as saturation and temperature) which approach in situ conditions.

Acknowledgements. This work was supported by National Science Foundation (NSF) grant DGE-9616038 to Saffer and by NSF grant OCE-0001871 to Marone. We thank two anonymous reviewers for their suggestions.

References

Bird, P., Hydration-phase diagrams and friction of montmorillonite under laboratory and geologic conditions, with implications for shale compaction, slope stability, and strength of fault gouge, *Tectonophysics*, 107, 235-260, 1984.

Brune, J., and R. Roy, Heat flow and stress along the San Andreas fault near Hollister, California, *Geol. Soc. Am. Special Paper* 121, 490, 1969.

Chester, F.M., and Logan, J.M., Composite planar fabric of fault gouge from the Punchbowl Fault, California, *J. Struct. Geol.*, 9, 621-634, 1987.

Colten-Bradley, V.A., Role of pressure in smectite dehydration: effects on geopressures and smectite-to-illite transformation, *Am. Assoc. Pet. Geol. Bull.*, 71, 1414-1427, 1987.

Fitts, T.G., and K.M. Brown, Stress-induced smectite dehydration: ramifications for patterns of freshening and fluid expulsion in the N. Barbados accretionary wedge, *Eart. Planet. Sci. Lett.*, 172, 179-197, 1999.

Hagin, P.N., Chang, C.T., and Zoback, M.D., Low-Temperature Viscous Deformation of Synthetic Fault Gouge, *EOS (Transactions)*, 1999 Fall Meeting Abstracts with Programs.

Logan, J.M., et al., Experimental studies of simulated fault gouge and their application to studies of natural fault zones, *in* Analysis of actual fault zones in bedrock, edited by R. C. Speed and R. V. Sharp, *U.S. Geol. Surv. Open File Rep.*, 79-1239, 305-343, 1979.

Logan, J.M., and K.A. Rauenzahn, Frictional dependence of gouge mixtures of quartz and montmorillonite on velocity, composition, and fabric, *Tectonophysics*, 144, 87-108, 1987.

Lupini, J.F., Skinner, A.E., and Vaughan, P.R., The drained residual strength of cohesive soils, *Geotechnique*, 31, 181-213, 1981.

Mair, K., and Marone, C., Friction of simulated fault gouge for a wide variety of velocities and normal stresses, *J. Geophys. Res.*, 104, 28899-28914, 1999.

Marone, C., and C. Scholz, The depth of seismic faulting and the upper transition from stable to unstable slip regimes, *Geophys. Res. Lett.*, 15, 621-624, 1988.

Marone, C., Laboratory-derived friction laws and their application to seismic faulting, *Annu. Rev. Earth Planet. Sci.*, 26, 643-696, 1998.

Morrow, C.A., D.E. Moore, and D.A. Lockner, The effect of mineral bond strength and absorbed water on fault gouge frictional strength, *Geophys. Res. Lett.*, 27, 815-818, 2000.

Morrow, C., B. Radney, and J. Byerlee, Frictional strength and the effective pressure law of montmorillonite and illite clays, *in* Evans, B. and T.F. Wong, (Eds.), Fault mechanics and transport properties of rocks; a festschrift in honor of W. F. Brace, San Diego, CA : Acad. Press, 69-88, 1992.

Reinen, L.A., J.D. Weeks, and T.E. Tullis, The frictional behavior of Lizardite and Antigorite serpentinites: Experiments, constitutive models, and implications for natural faults, *Pageoph*, v. 143, 317-358, 1994.

Rice J.R., Fault stress states, pore pressure distributions, and the weakness of the San Andreas Fault, *in* Evans, B. and T.F. Wong, (Eds.), Fault mechanics and transport properties of rocks; a festschrift in honor of W. F. Brace, San Diego, CA : Acad. Press, 475-504, 1992.

Scholz, C.H., Earthquakes and friction laws, *Nature*, 391, 37-42, 1998.

Segall, P., and J.R. Rice, Dilatancy, compaction, and slip instability of a fluid infiltrated fault, *J. Geophys. Res.*, 100, 22155-22173, 1995.

Shimamoto, T., and J.M. Logan, Effects of simulated clay gouges on the sliding behaviour of Tennessee sandstone, *Tectonophysics*, 109, 165-175, 1981.

Vrolijk, Peter, and B.A. van der Pluijm, Clay Gouge, *J. Struct. Geol.*, 21, 1039-1048, 1999.

Wang, C.Y., N. Mao, and F.T. Wu, Mechanical properties of clays at high pressure, *J. Geophys. Res.*, 85, 1462-1468, 1980.

Zoback et al., New evidence on the state of stress of the San Andreas Fault system, *Science*, 238, 1105-1111, 1987.

K. Frye, Department of Earth, Atmospheric, and Planetary Sciences, Massachusetts Institute of Technology, 54-724, Cambridge, MA 02139 (kfrye@barre.mit.edu.)

K. Mair, Department of Earth Sciences, University of Liverpool, Liverpool L69 3GP, UK.

C. Marone, Department of Geosciences, The Pennsylvania State University, University Park, PA 16802.

D. Saffer, Department of Geology and Geophysics, University of Wyoming, 16th and Gibbon St., Laramie, WY 82071-3006 (dsaffer@uwyo.edu.)

(Received January 16, 2001; revised March 19, 2001; accepted April 12, 2001.)